SCIENTIFIC REPORTS

OPEN

SUBJECT AREAS:
PATHOGENESIS
MEDICAL RESEARCH

Received
6 March 2014

Accepted
28 August 2014

Published
18 September 2014

Correspondence and requests for materials should be addressed to K.R.-T. (Kristina.Rydell-Tormanen@med.lu.se)

Absence of fibromodulin affects matrix composition, collagen deposition and cell turnover in healthy and fibrotic lung parenchyma

Kristina Rydell-Törmänen[1], Kristofer Andréasson[2], Roger Hesselstrand[2] & Gunilla Westergren-Thorsson[1]

[1]Dept. Experimental Medical Science, Lund University, Lund, Sweden, [2]Dept. Clinical Sciences, Section of Rheumatology, Lund University, Lund, Sweden.

The ECM exerts great effects on cells, and changed composition may therefore have profound impact. Small leucine-rich proteoglycans, e.g. fibromodulin, are essential in collagen assembly. Our aim was to investigate the role of fibromodulin in healthy and fibrotic lung parenchyma, theorizing that fibromodulin-deficient animals would be protected against fibrosis. Repeated subcutaneous bleomycin-injections were given to wild type and fibromodulin-deficient mice, inducing pulmonary fibrosis. Development of fibrosis, ECM composition, cell turnover and inflammatory responses were investigated. Fibromodulin-deficient animals were not protected from fibrosis, but the composition of the matrix was affected, with decreased Collagen I in fibromodulin-deficient animals, both in controls (0.07 ± 0.04% vs. 0.18 ± 0.07% tissue area) and after bleomycin (0.37 ± 0.16% vs. 0.61 ± 0.21% tissue area). Biglycan was increased in fibromodulin-deficient animals, whereas decorin was decreased. Furthermore, bleomycin increased cell turnover in wild type, but only proliferation in fibromodulin-deficient animals, resulting in hyperplasia. In addition, the bleomycin-induced immune response was affected in fibromodulin-deficient animals. We thus conclude that fibromodulin has a profound effect on ECM, both in healthy and fibrotic lung parenchyma, and may be providing a permissive microenvironment affecting cell turnover. Furthermore, this study highlights the need to acknowledge specific ECM components, when assessing tissue properties and ultimately cell behaviour.

Pulmonary fibrosis is characterized by increased deposition of ECM, and it is well known that the ECM and its composition and biomechanical properties have profound effects on cell differentiation, proliferation and protein synthesis[1–4]. In fibrosis, the entire matrix composition is affected, yet most studies focus on collagen and collagen cross-linking. The important role of other matrix components such as the small leucine-rich proteoglycans (SLRPs), which are important in collagen assembly and by association for tissue biomechanics, as well as for sequestering chemokines such as pro-inflammatory cytokines and growth factors, has largely been neglected.

The fibrillar collagens I and III are the most prominent types of collagen in the lung[5–7]. Fibrillar collagen is cross-linked by lysyl oxidase (LOX), and multiple fibrils form collagen fibres. A correct collagen assembly is necessary to avoid collagenolysis[8], and SLRPs play an essential role in this process[9–13]. It is known that absence of SLRPs has severe effects on collagen fibrillation and overall SLRP balance[9,14–18] throughout the body, although the situation within lungs has been sparsely investigated and knowledge is mostly lacking. We used fibromodulin-knock out animals (FM) to investigate the role of fibromodulin-deficiency in healthy and fibrotic lung parenchyma. Fibrosis was induced by repeated subcutaneous (SC) bleomycin-injections, as previously described[19]. Importantly, in contrast to most other studies, the SC administration results in a homogenous fibrosis mainly affecting lung parenchyma. We were therefore able to perform a unique study, focusing on a specific niche in the lung: the parenchyma, excluding large airways and vessels.

The aim of our study was therefore to study the role of fibromodulin in healthy and fibrotic lung parenchyma, investigating the effects on development of fibrosis, collagen fibrillation, cell behaviour and inflammatory responses. We theorized that fibromodulin-deficient animals would be somewhat protected against fibrosis, due to less efficient collagen assembly.

Based on our results, we conclude that fibromodulin-deficiency has severe effects on the *composition* of the matrix in both healthy and fibrotic lung parenchyma, but does not protect the lungs from developing pulmonary fibrosis. Fibromodulin-deficiency did not affect the tissue density and total ECM, but increased LOX, biglycan, collagen I and cell turnover. We found bleomycin administration to result in mismatched cell turnover, increasing cell density, as well as having an effect on the immune response. We thus conclude that fibromodulin have a significant impact on the ECM in lung parenchyma, and may be providing a permissive microenvironment affecting cell turnover and matrix composition.

The ability of ECM to affect cellular processes is becoming increasingly clear, and this study highlights the need to acknowledge specific ECM components, such as proteoglycans, when assessing tissue properties and cell behaviour.

Results

Animal model. No fatalities occurred within the study, and the body weight did not decrease in any of the four groups, furthermore no behavioural differences were seen between any of the groups. It is however possible that bleomycin has physiological effects, not seen in caged mice. No sign of emphysema or other lung disorders were seen in FM controls compared to WT controls.

Parenchymal fibrosis and systemic TGF-β. Total collagen (Masson's Trichrome/MTC) was significantly increased in both fibrotic WT ($p = 0.0004$) and FM ($p < 0.0001$) compared to their respective controls (Figure 1A). No difference was found when comparing genotypes, i.e. fibromodulin deficiency had no effect on bleomycin's ability to induce fibrosis.

Fibrillar collagen (Picrosirius Red/PSR) increased following bleomycin administration in WT ($p = 0.0008$, Figure 1B). In the FM bleomycin group, bleomycin failed to induce an increased PSR labelling (significantly less PSR positivity compared to WT), but FM controls displayed a significantly ($p = 0.0131$) more intense labelling compared to WT-controls, suggesting more thick collagen fibrils at baseline in FM. Illustrative images of PSR staining in the four groups are found in Figure 2A–D.

We furthermore investigated the density of the lung (Figure 1C), i.e. the proportion of the lung occupied by tissue. The density was found to be in accordance with total collagen (MTC): bleomycin induced a significantly increase tissue density in both WT ($p < 0.0001$) and FM-ko ($p = 0.0011$) compared to their respective controls. No difference between the control groups was found, which suggests that fibromodulin-deficiency itself does not induce pulmonary fibrosis.

As bleomycin is administered systemically, we investigated the presence of TGF-β in serum (sTGF-β, Figure 1D). We found a small, but statistically significant increase in sTGF-β in WT following bleomycin administration, but not in FM. This suggests that fibromodulin-deficiency do not cause decreased TGF-β sequestering, making the animals more prone to develop fibrosis.

Fibromodulin is involved in collagen fibrillation and we therefore investigated expression of the most prominent fibrillar collagens in the lung: types I and III (Figure 1E and F). Collagen I was highly affected by bleomycin, and increased 3-fold following bleomycin-administration ($p = 0.0001$) in WT and 4-fold ($p < 0.0001$) in FM (Figure 1E, Figure 2E–H). Moreover, FM showed significantly less collagen I in both controls ($p = 0.0062$) and bleomycin-treated ($p = 0.0179$) animals. In contrast to collagen I, collagen III appeared to be unaffected by both bleomycin, and fibromodulin-deficiency, as no differences were found (Figure 1F).

The amount of cross-linking of the collagens has been ascribed an important role for development and reversibility of fibrosis, and we therefore investigated the presence of LOX-positive staining (Figure 1G). Our results show significantly higher levels of LOX in FM controls compared to WT controls ($p = 0.0203$) and FM bleomycin compared to WT bleomycin ($p = 0.0115$) compared to WT. Bleomycin administration significantly increased LOX expression compared to respective control group.

Expression of other SLRPs; lumican, biglycan and decorin. Lumican is described to be up regulated in tendons of FM-ko[9], and we therefore investigated the expression in lungs (Figure 3A, Figure 2I–L). Interestingly, we found that the lumican expression was significantly lower ($p = 0.0003$) in FM controls compared to WT controls. Bleomycin administration resulted in a markedly decreased lumican expression in WT, whereas no change was found in FM. The expression of decorin (Figure 3B, Figure 2M–P) was significantly lower in FM controls, compared to WT controls ($p = 0.0231$). This study focused on the lung parenchyma, and we noted that positive decorin and lumican staining was predominantly found in a perivascular and peribronchial pattern.

In contrast to the other SLRPs, Biglycan was significantly increased in fibrotic lungs ($p < 0.0001$) (Figure 3C, Figure 2Q–T), and was affected by lack of fibromodulin such that FM controls displayed significantly higher levels of biglycan compared to WT ($p = 0.0262$). The biglycan-positive labelling was found throughout the lung parenchyma (Figure 2I–L), in addition to a perivascular and peribronchial distribution similar to decorin and lumican.

To investigate whether the increased expression of biglycan was due to increased synthesis, we performed RT-qPCR. The results showed no significant transcriptional effects (Figure 3D).

Cell turnover. Analysis of total proliferation (Figure 4A) showed a significantly increased proliferation in both WT and FM following bleomycin-administration ($p < 0.0001$ in both). In addition, FM controls displayed a significantly increased proliferation-rate compared to WT controls ($p < 0.0001$), and this increased proliferation was present also following bleomycin-administrations. Proliferating cells were found evenly throughout the lung parenchyma (Figure 5A–D), and to assess the type of proliferating cells, we performed double stainings. The results showed proliferating alveolar epithelial type I cells to be most common (Figure 5I–J), in addition to scattered endothelial cells, alveolar epithelium type II cells, pericytes and smooth muscle cells, whereas no proliferating CD45-positive cells was found. We did however note proliferating cells that were negative for the different cell-specific markers; we concluded a large proportion of these to be fibroblasts (based on lack of labelling and localization). Intriguingly, proliferating cells were often found in association with small vessels, primarily located on the outside of the vessel (Figure 5K–L).

The number of apoptotic cells (Figure 4B) was higher in WT bleomycin ($p < 0.0001$) compared to WT controls. Apoptosis was also increased in FM controls ($p = 0.0027$) compared to WT controls, suggesting an increased cell turnover. In contrast, FM bleomycin did not show any increased apoptosis following bleomycin, suggesting a mismatched turnover. Apoptotic cells were found evenly distributed throughout the lung (Figure 5E–H), and double stainings revealed them to be mainly alveolar type I cells (AP5, Figure 5M) and fibroblasts (using the same definition as for proliferating fibroblasts, described above). Scattered apoptotic endothelial cells (CD31) and neutrophils were also found, but no apoptotic alveolar type II cells or pericytes were detected.

To investigate if the mismatched turnover (proliferation vs. apoptosis) resulted in increased cell density, we quantified the number of nuclei in tissue and related this to area (Figure 4C). The results showed that the total cell number remained fairly consistent in WT, despite bleomycin-administration, whereas the total number of nuclei was significantly higher in FM bleomycin compared to WT bleomycin ($p = 0.0462$).

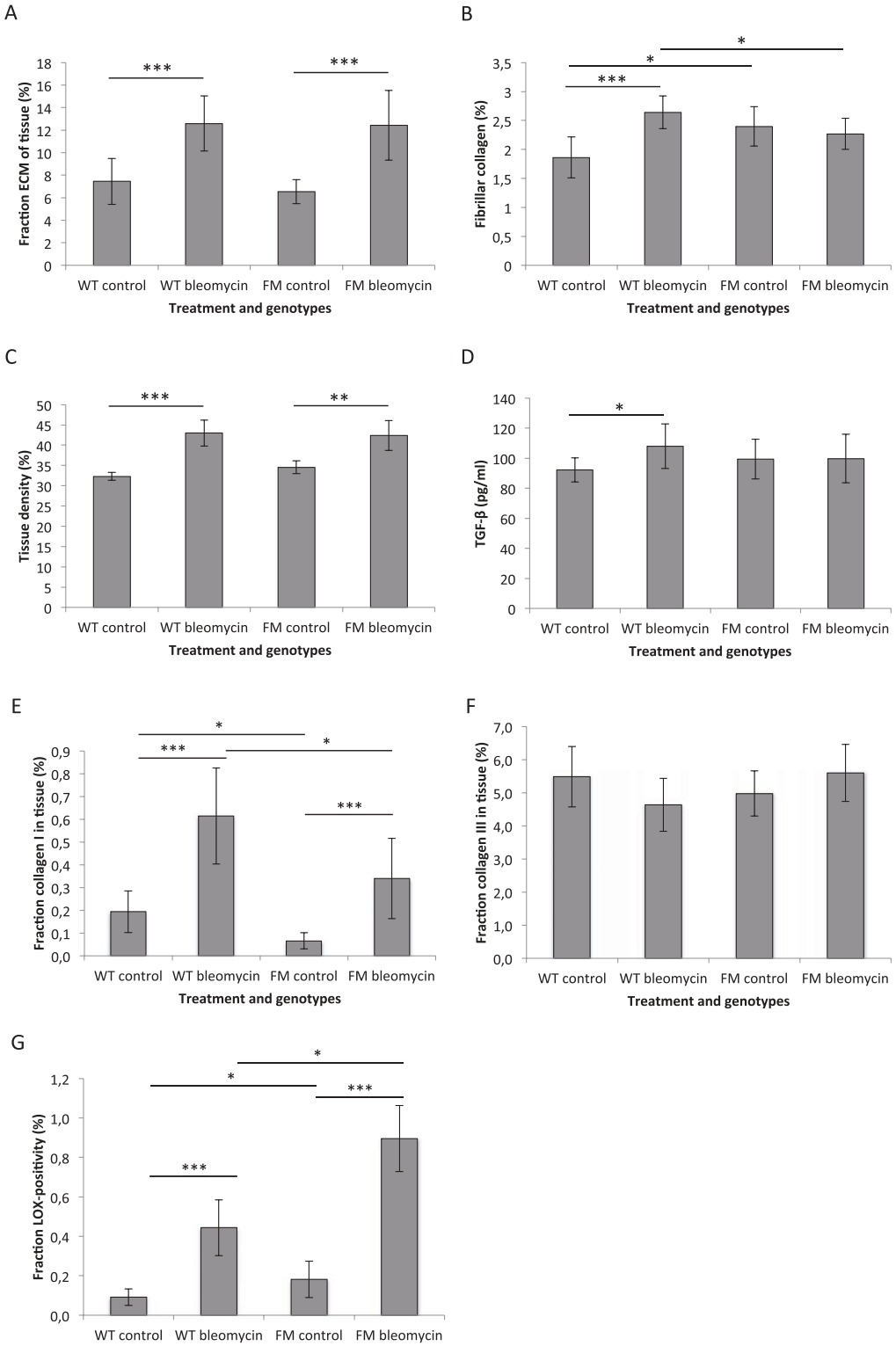

Figure 1 | Parenchymal fibrosis and systemic TGF-β. ECM is increased in response to bleomycin in both wild types (WT) and fibromodulin deficient (FM) animals (A). The fraction of fibrillar collagen, determined by Pricrosirius Red (PSR) was significantly increased in WT following bleomycin-administrations, whereas FM did not display any increase (B). In addition, a significantly increased fraction fibrillar collagen was found in FM-Controls compared to WT-Controls. The tissue density was increased following bleomycin-administrations in both genotypes (C). The level of TGF-β in serum (D) was significantly increased following bleomycin administrations in WT, but not in FM. The fraction of collagen I (E) was significantly increased in both genotypes following bleomycin-administrations, but significantly less collagen I was found in both healthy and fibrotic FM compared to WT. In contrast to collagen I, collagen III (F) showed no difference between different treatments of genotypes. Levels of LOX (G) were increased in FM compared to WT, and increased following bleomycin administrations in both genotypes. Tissue density is given as fraction tissue of total lung parenchyamal area (%), excluding the air spaces, TGF-β as pg/ml and all other data is given as fraction labelled area of tissue area (%). A minimum of 5 animals/group was analysed. Data is given as mean ± SD, statistical analysis is preformed by the Kruskal-Wallis test, with LSD post hoc and * = $p < 0.05$, ** = $p < 0.01$ and *** = $p < 0.001$.

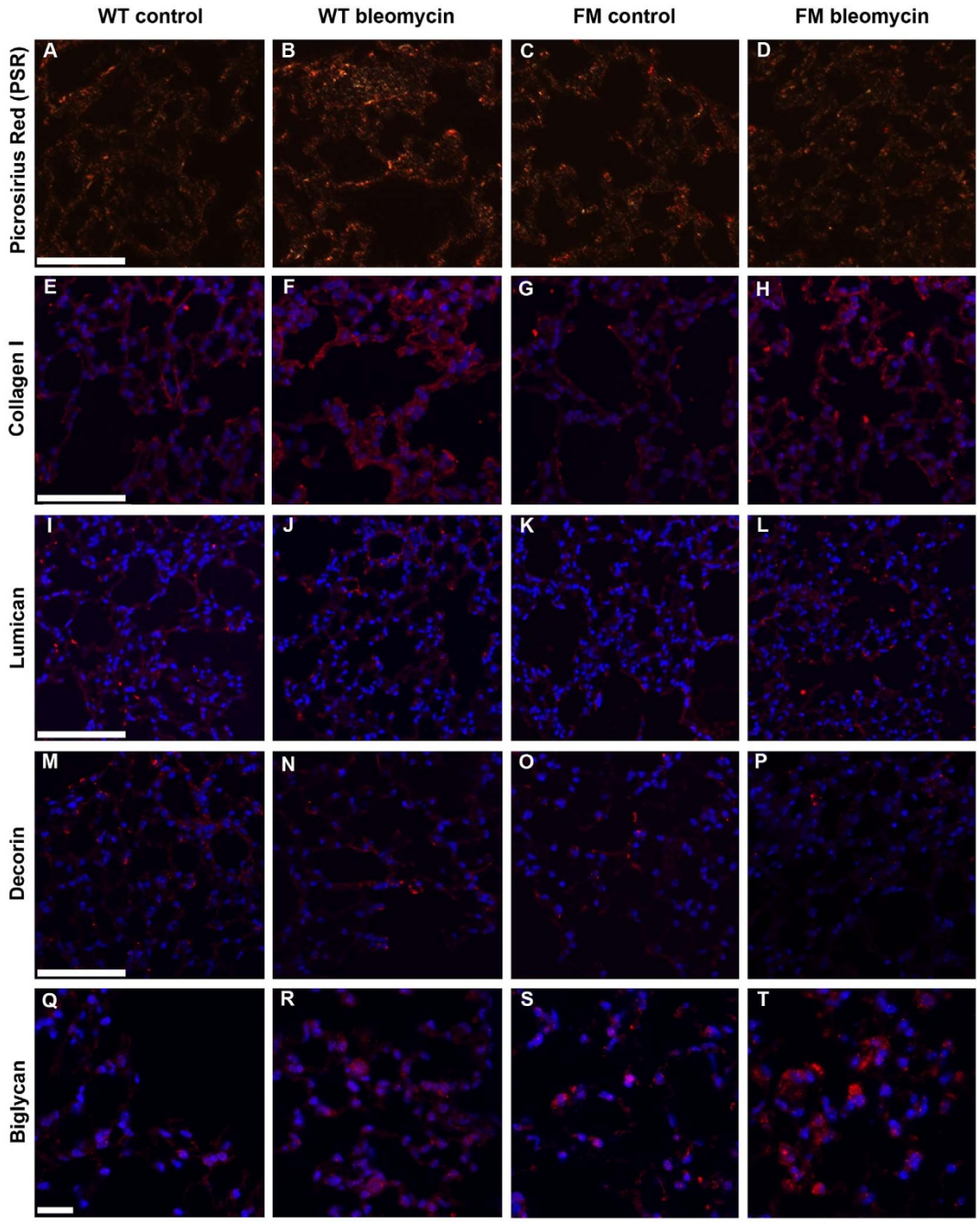

Figure 2 | Representative images of parenchymal fibrosis. Illustrative images of different stainings of different groups; Picrosirius Red/PSR (A–D), Collagen I (E–H), Lumican (I–L), Decorin (M–P) and Biglycan (Q–T). 4.5 μm thick paraffin-embedded sections were stained according to standard protocol, previously described. Scale bar denotes 100 μm in (A–D) and (I–L), 50 μm in (E–H) and (M–P), and 20 μm in (Q–T).

Local immune responses and systemic inflammation. To investigate the parenchymal inflammation, and seeking to determine if immune cells could be represent the increased cell numbers found in lungs of fibrotic FM, we quantified the number of neutrophils and macrophages in tissue. A slight neutrophilia was found in WT, but not in FM following bleomycin administration (Figure 6A). The results showed the number of macrophages to be significantly higher ($p < 0.001$) in bleomycin-treated fibromodulin deficient animals, compared to FM control and WT bleomycin (Figure 6B).

We therefore decided to quantify the concentration of MCP-1, which is a major macrophage chemotactic cytokine, in serum (Figure 6C). The results showed that MCP-1 occurred in the highest concentration in WT controls. FM controls and WT bleomycin had significantly lower concentration ($p < 0.05$) MCP-1 in blood. FM bleomycin displayed a highly variable MCP-1 concentration in blood. This may indicate that no active recruitment of macrophages is on going at this time (4 w), and the increased macrophages found in lung parenchyma likely represent cells left from an inflammatory response.

As bleomycin is administered systemically, we decided to investigate inflammatory cytokines in serum, using a protein array (Figure 6D). The results suggest that systemic bleomycin have some effects on the cytokine profile in serum, as bleomycin treated animals showed weak but positive staining for IFNγ, IL-1ra, M-CSF, MCP-1, MIG and TIMP-1, in addition to C5a and CD54 (encircled by dotted lines) which is found in all animals. The expression varied somewhat depending on genotype, and FM bleomycin appeared to express more cytokines than WT bleomycin.

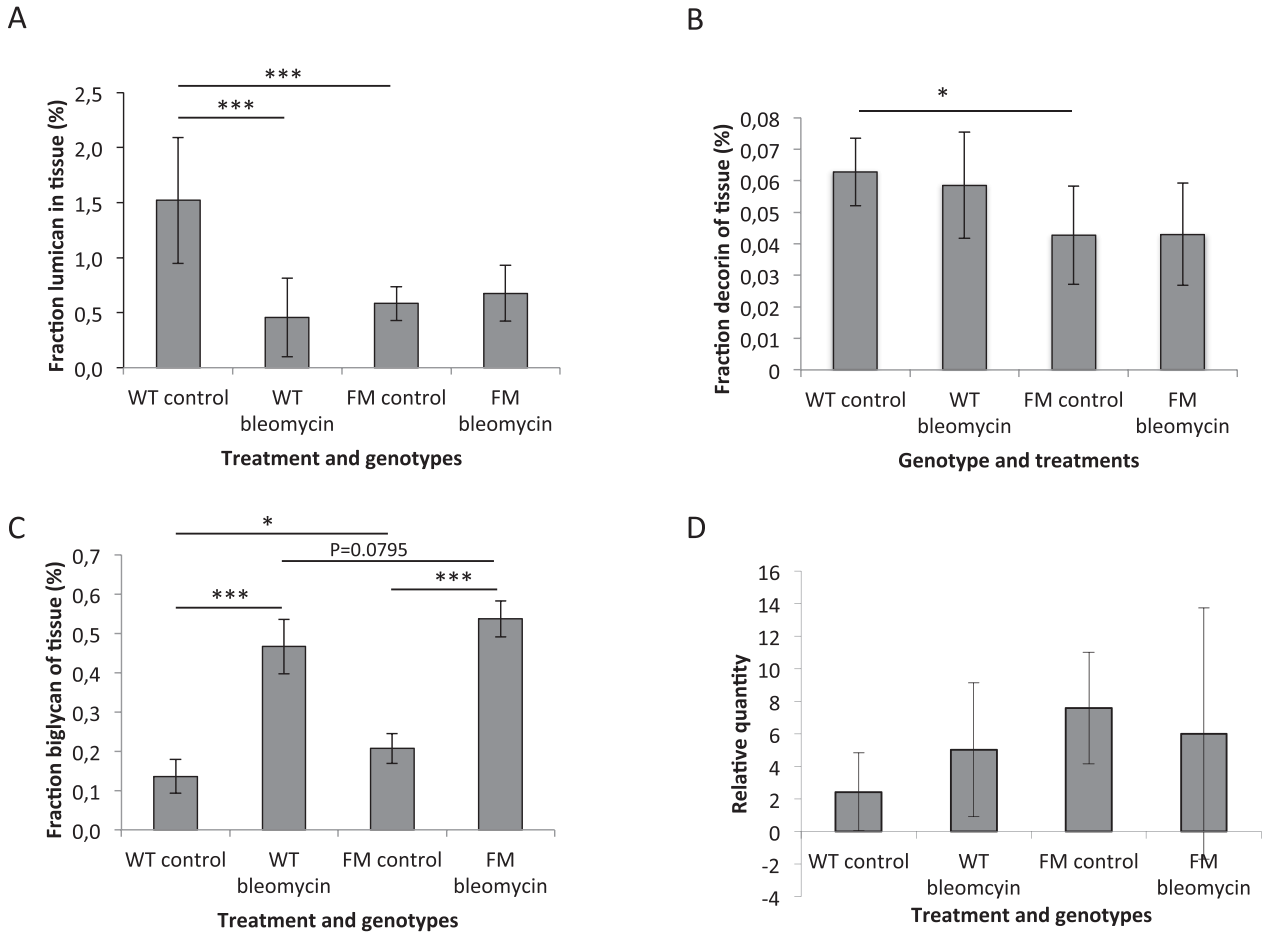

Figure 3 | Expression of the other SLRPs decorin, biglycan and lumican. Lumican (A) was significantly decreased in wild types (WT) receiving bleomycin, and in fibromodulin deficient (FM) controls, whereas no difference was found between healthy and fibrotic FM. Decorin expression (B) was significantly lower in FM, whereas no difference in either genotype was found following bleomycin-injections. In contrast to lumican and decorin, bleomycin increased biglycan expression in both genotypes (C), and FM-Controls showed higher expression than WT-Controls. Although not statistically significant, a similar pattern was found comparing bleomycin treated groups. Analysis of mRNA expression (D) showed no increased biglycan transcription in FM or following bleomycin administration. The different SLRPs are given as fraction tissue of total lung area (%), and mRNA was determined as 2Exp. A minimum of 5 animals/group were analysed. Data is given as mean ± SD, statistical analysis is preformed by the Kruskal-Wallis test, with LSD post hoc and * = $p < 0.05$, ** = $p < 0.01$ and *** = $p < 0.001$.

Discussion

To the best of our knowledge, we here present the first characterization and description of the role of fibromodulin-deficiency in healthy and fibrotic lung parenchyma. This study uniquely focuses on a single niche of the lung: the lung parenchyma, excluding large airways and vessels. The absence of fibromodulin results in an altered matrix composition, affecting collagens and proteoglycans, as well as cell behaviour and inflammatory pattern. The importance to acknowledge SLRPs when investigating ECM is becoming increasingly clear.

We theorized that fibromodulin-deficiency might have a somewhat protective effect against fibrosis, as incorrectly assembled collages would be more prone to degradation and thus less collagen would be deposited in the tissue. Our results however, contradict this and instead suggest that fibromodulin-deficiency have an effect on the composition of the matrix. Collagen I, other SLRPs and cell turnover was highly affected by fibromodulin-deficiency, and it can be speculated that these alterations are interconnected; collagen assembly is highly dependent on SLRPs and cell behaviour is affected by tissue stiffness, which is affected by collagen and collagen cross-linking. The altered composition may also have clinical effects, e.g. vital capacity, which was not explored further due to the difficulties to accurately measure subtle changes in lung function. We are however currently exploring the possibility to use atomic force microscopy in determining elasticity and stiffness of lungs. Furthermore, the composition of the ECM may affect cell migration, for example by immune cells during inflammation. It is thus clear that deletion of a normally low-expressed ECM component may have pervasive effects on physiological processes.

A rough analysis of total fibrillar collagens was performed by the well-established but somewhat blunt technique of Picrosirius Red (PSR). Importantly, using PSR and polarized light, thinner fibres appear pale yellow to green, and for technical reasons we are less effective in detecting the pale yellow labelling. For a more specific investigation, we therefore quantified collagen type I and III specifically as well as LOX, and found that Collagen I was significantly higher and LOX significantly lower in WT controls compared to FM controls, indicative of low collagen turnover. In contrast, fibromodulin-deficient animals have low expression of Collagen I but high expression of LOX, indicative of a more rapid turnover, likely due to improper fibrillation, these fibres are less resistant to collagenolysis and is thus degraded to a higher extent, which increases the rate of turnover.

The increased PSR positivity found in FM controls may be attributed to collagen assembly assisted by another SLRP. Our results show biglycan to be significantly increased in fibromodulin-deficient ani-

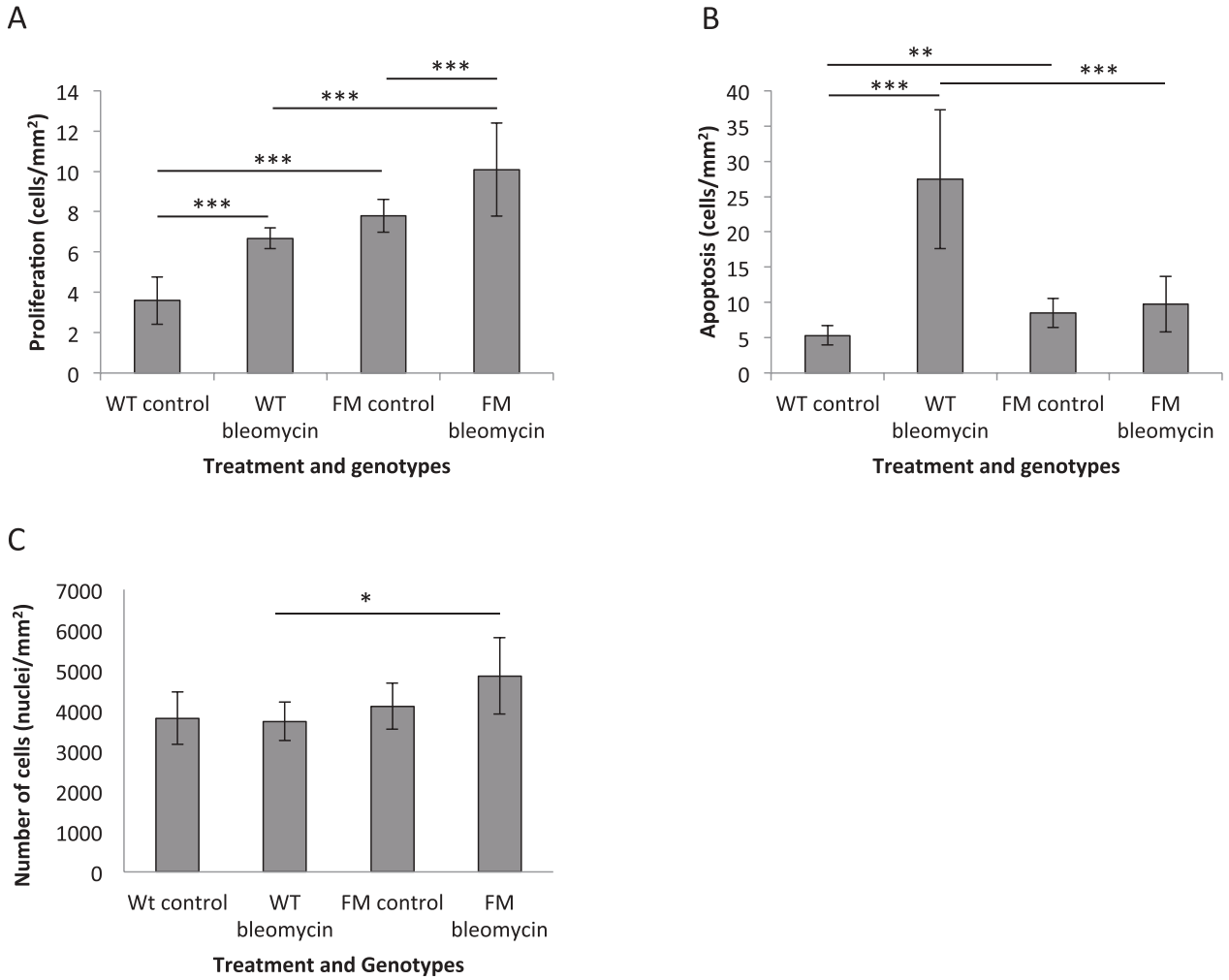

Figure 4 | Proliferation, apoptosis and number of nuclei. Total number of proliferating cells (A) increased following bleomycin-administration, in both genotypes, and fibromodulin-deficient animals had increased number of proliferating cells in both controls and fibrotic lungs compared to WT. The number of apoptotic cells (B) was increased in WT, but not FM, following bleomycin administrations, as well as in FM controls compared to WT controls. The bleomycin-induced increased proliferation was balanced by an increased apoptosis in wild types (WT), but not in FM (B). As a result, the total number of nuclei (C) is significantly increased in bleomycin-injected FM compared to bleomycin-treated WT. Proliferation was determined by counting the number of positive cells (PCNA in proliferation and TUNEL in apoptosis), and relating this number to tissue area. Total number of nuclei was obtained by counting nuclei and relating this to tissue area. A minimum of 6 animals/group were analysed. Data is given as mean ± SD, statistical analysis is preformed by the Kruskal-Wallis test, with LSD post hoc and * = $p < 0.05$, ** = $p < 0.01$ and *** = $p < 0.001$.

mals, and it is plausible to suggest that biglycan assists in collagen fibrillation in the absence of fibromodulin. It is also possible that FM have a higher expression of fibrillar collagens, which may represent a compensatory increase during normal conditions, but in a fibrotic situation this back up-mechanism might be unable to cope. This may be supported by findings in fibromodulin controls, where collagen I expression is significantly lower than WT, but the amount of fibrillar collagens is increased.

Fibromodulin-deficiency had effects on expression of other SLRPs, Lumican that is increased in tendons of fibromodulin-deficient animals[9], whereas we found it to be decreased, suggesting compensatory mechanisms to be tissue specific. The increased expression of biglycan and decreased expression of decorin is intriguing as both have extensive cellular effects. Decorin is anti-proliferative[20,21], whereas Biglycan is anti-apoptotic[22,23], and it is likely that fibromodulin has similar properties. This is supported by a recent study in fibromodulin-deficient animals, describing increased proliferation, but not apoptosis, after aortic shear stress, resulting in increased cell density[24].

Proliferating cells were found throughout the lung parenchyma, evenly distributed irrespectively of genotype. Our investigation showed a large proportion of the proliferating cells to be alveolar type I cells, but we also detected scattered proliferating cells of other types, including endothelial cells. This was unexpected as the endothelium is exposed to bleomycin, we expected a large number of proliferating endothelial cells. It is likely however that proliferating endothelial cells is an early event, and epithelial proliferation represents a later state, with fibrosis spreading to adjacent tissue. In addition to proliferating cells, apoptotic cells were found throughout the lung parenchyma, and in similarity to proliferating cells, a large proportion were alveolar epithelium type I cells. We did note proliferating and apoptotic cells that were negative for the cell specific markers, and concluded a large proportion of these to be fibroblasts of various types.

It can be argued that the increased cell numbers found in FM bleomycin is immune cells, for example neutrophils and/or macrophages. Our results however suggest this to be unlikely. The slightly increased number of macrophages in FM bleomycin is more likely to represent a delayed (compared to WT) immunological process; deficient animals appear to have a delayed resolution of the bleomycin-induced inflammation. This is supported by our data on sMCP-1,

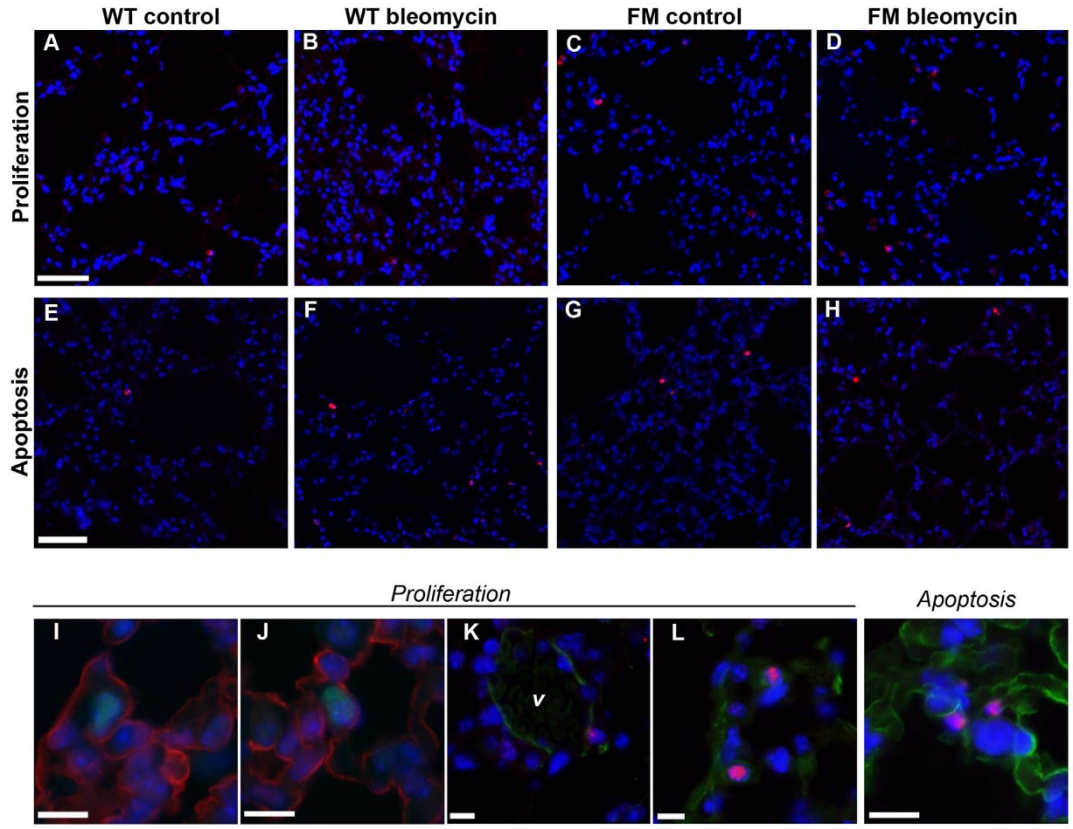

Figure 5 | Illustrative images of proliferating and apoptotic cells in lung parenchyma. Proliferating cells (A–D) were found evenly throughout the lung parenchyma, as were apoptotic cells (E–H). To investigate the type of proliferating cells we performed double-stainings; Proliferating alveolar epithelial type I cells (I–J) were visualized using an antibody directed against PCNA (green), and staining for Aquaporin 5 (AP5, red) and proliferating blood vessel (*v*) associated cells (K–L) were visualized by PCNA (red) and CD31 (green). Apoptotic alveolar epithelial type I cells were visualized by TUNEL (red) and AP5 (green). DAPI (blue) was used as nuclear stainings in all protocols. Scale bar denotes 50 μm in (A–H), and 10 μm in (I–M).

which indicates that no active macrophage recruitment is on going in the FM bleomycin animals. The elucidation of specific effects of fibromodulin-deficiency on inflammation is beyond the scope of this study, but speculatively, fibromodulin may have effects on inflammation by altering mechanical properties of the connective tissue and thus interfering with immune cell trafficking, or affect levels of inflammatory cytokines within the ECM.

Our results from the protein array shows that bleomycin have systemic effects on serum cytokines, evident by the effects on IFNγ, IL-1ra, M-CSF, MCP-1, MIG and TIMP-1. As the array was made after 4 w of bleomycin administrations, it is likely to represent a sub-chronic response, rather than acute effect of bleomycin. It is also important to emphasize that only one animal from each group were analysed and the array thus represents a snapshot of a process extending over several weeks.

To the best of our knowledge, no methodical quantification or description of aging fibromodulin-deficient mice has been published. In this study animals were sacrificed at 19 weeks of age, which is adult but not aged animals. At this time no phenotypic differences of the lungs was found, and a preliminary study on aged mice did not show any apparent differences (such as fibrosis or emphysema) between genotypes.

Based on our results we conclude that fibromodulin has a profound effect on the extracellular matrix, both in healthy and fibrotic lung parenchyma, and may be providing a permissive microenvironment affecting cell turnover and matrix composition. The importance of ECM in cellular processes is becoming increasingly clear, and this study thus highlights the need to acknowledge specific ECM components, such as proteoglycans, when assessing tissue properties and ultimately cell behaviour.

Methods

Mice. Fibromodulin-deficient (FM) and wild types (WT) were a kind gift from Å. Oldberg[9]. Animals were kept under barrier conditions, with food and water *ad libitum*. All methods were carried out in accordance with approved guidelines and approved by the local ethics committee (Malmö/Lund, Sweden; number M275-10). For the experiments 15-week (w) old females were used. Based on treatment and genotype, four groups were formed: WT-controls, WT-bleomycin, FM-controls and FM-bleomycin (Table 1). 6–10 animals were included in each group. Animals included were genotyped as previously described[25].

Bleomycin administration and sacrifice. We utilized a modified model of bleomycin-induced pulmonary fibrosis, previously described[19]. Briefly, 0.1 ml bleomycin (0.5 mg/ml, Bleomycinsulphate, Bleomycin Baxter, Baxter Medical AC, Kista, Sweden) was administered subcutaneously on the back, three times a week for 4 w, a total of 12 injections and a total bleomycin dose of 24 mg/kg. Control animals received saline injections administered according to the same protocol, although previous experiments have shown no difference between saline-injected and naïve animals (data not shown). Animals were sacrificed within 48 h of the last injection, lungs were inflated with 2–2.5 ml PBS and lung tissue samples were obtained. Tissue was fixed in 4% formaldehyde, dehydrated and embedded in paraffin; 4,5 μm slices were used.

Collagen stainings. Two different methods were used to quantify collagen content in the tissue: Picro Sirius Red (PSR, visualizing fibrillar collagen as birefringent structures under polarized light) and Masson Trichrome (MTC, labelling connective tissue, primarily collagens, blue). Both stains were performed using standard protocols: *PSR*: Sections were rehydrated and stained with Picro Sirius Red (PSR, Direct Red 80, Alfa Aesar, Karlsruhe, Germany) according to standard protocol. *MTC*: Sections were rehydrated and stained according to manufacturers protocol (MTC, Masson Trichrome Kit, Sigma-Aldrich, St. Louis, MO, USA).

Immunohistochemistry (IHC). Primary antibodies directed against the following was used within the study (technical details are found in table 2): biglycan, collagen I, collagen III, decorin, lumican, PCNA, LOX, neutrophils and macrophages (F4/80). For investigation of proliferating and apoptotic cells, antibodies against the following was used in double stainings with TUNEL and PCNA; Smooth muscle cells (α-SMA, proliferation only), alveolar epithelial type I cells (Aquaporin5/AP5), endothelial cells

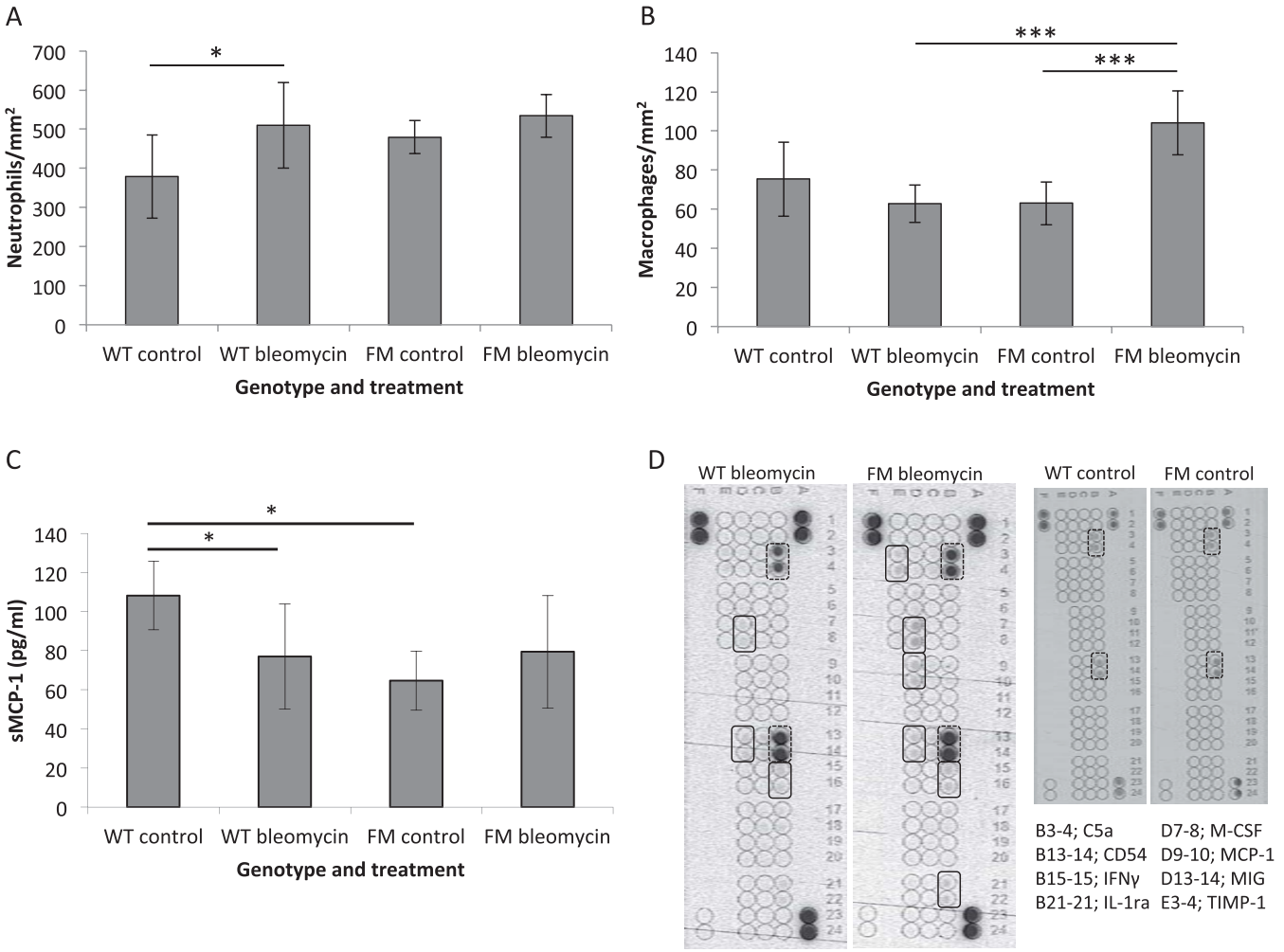

Figure 6 | Local immune responses and systemic inflammation. A slight neutrophilia was found (A) in WT but not FM following bleomycin. In contrast, the number of macrophages was significantly increased in FM bleomycin compared to FM controls and WT bleomycin (B). We investigated the level of MCP-1 in serum (C) and found that MCP-1 occurred in the highest concentration in WT controls. FM controls and WT bleomycin had significantly lower concentration and FM bleomycin displayed a highly variable MCP-1 concentration. To investigate systemic inflammatory cytokines at this time a protein array was performed (D), showing the presence of several inflammatory mediators (encircled) in bleomycin-treated animals whereas only two (c5a and CD54, dotted lines) were also found in controls.

(CD31), cells of hematopoietic origin (CD 45 (PCNA only)), Neutrophil (TUNEL only), pericytes (NG2) and alveolar epithelial type II cells (Prosurfactant protein C/ProSPC).

The IHC was performed according to a standard protocol. Briefly, sections were rehydrated and allowed to equilibrate in TBS for 15 minutes, followed by a pre-treatment if necessary. Next, the primary antibody was applied for 1.5–2 h (RT) or over night at 4°C. Slides were rinsed and secondary antibodies in addition to DAPI were applied for 1 h. The secondary antibodies (Alexa 488 or Alexa 555 both from Molecular Probes Life Technologies, Carlsbad, CA, USA) were diluted 1 : 200, as was DAPI (30 μM). Slides were mounted in fluorescent mounting medium and stored in −20°C before analysis. Apoptosis was detected by TUNEL (ApopTag Red In Situ, S7165, Merck Millipore, Solna Sweden) according to the manufacturer's instructions.

Analysis of cytokines in serum. A protein array (Mouse Cytokine Antibody Array, Panel A, ARY006, R&D Systems, Minneapolis, MN, USA) was used to screen the presence of a large number of pro-inflammatory cytokines in serum. Serum from one animal from each group was subjected to analysis, which was performed according to the manufacturers instructions.

Table 1 | Matrix illustrating treatments and genotypes within the study

Genotype \ Treatment	Saline	Bleomycin
Wild type (WT)	WT control	WT bleomycin
Fibromodulin-deficient (FM-ko)	FM control	FM bleomycin

To determine the concentration of MCP-1/CCL2/JE and TGF-β in serum (n = 5–6) was investigated by ELISAs MJE00 (MCP-1/CCl2/JE, R&D Systems), and MB100B (TGF-β, R&D Systems), both according to the manufacturer's protocols.

RNA extraction, DNA synthesis and RT-PCR. Tissues were snap frozen for later extraction of total RNA using RNeasy (Qiagen GmBH, Hilden, Germany) according to the manufacturer's instructions. The quantity of RNA was measured by spectrophotometry using a NanoDrop 2000c (Thermo Fisher Scientific, Gothenburg, Sweden). Total RNA (1 μg) was reverse-transcribed using superscript II according to manufacturers manual (Invitrogen, Carlsbad, CA, USA) and stored at −70°C.

5 μl cDNA (diluted 1 : 250) was mixed with 15 μl SYBR-green PCR master mix (Applied biosystems, Life Technologies) and amplified by RT-qPCR using Agilent Technologies (Santa Clara, CA, USA). The samples were held for 10 minutes at 95°C, before being cycled for 40 cycles of 30 s at 95°C, 1 min at 59°C and 1 min at 72°C. Each sample was analysed in triplicate. Reactions were performed using MX3000P 96 well plates (Agilent Technologies). Primers detecting biglycan were constructed by, and ordered from Sigma Aldrich. The following were used; Biglycan_S TCCTCCAGGTTGTCTATCT, Biglycan_AS TTGACTCCGAAGCCCATA.

Digital imaging and analysis of histology. Histological analyses were performed by digital imaging and the software ImageJ (v1.44j; Wayne Rasband, NIH, USA). All slides were analysed in a blinded fashion and images of the lung parenchyma were obtained randomly. To assure imaging of the regions of interest and consistency between samples, we selected the bottom part of the section close to (directly under) the pleura as a starting point for each image. From this starting point, the next image was taken 2–4 image fields right and 1–3 upwards from the starting point. A variable number of images of each slide were taken, ranging from 4 (when obtained at 20×

Table 2 | Technical details regarding the antibodies used within the study

Antigen	Product #	Source	Dilution	Pretreatment
α-SMA	C6198	Sigma-Aldrich	1 : 2000	Proteinase K
Aquaporin5	ab78486	Abcam	1 : 500	Proteinase K
Biglycan	ab58562	Abcam	1 : 100	Chon. ABC + Prot. K
CD31	ab56299	Abcam	1 : 100	Proteinase K
CD45	ab25386	Abcam	1 : 300	Proteinase K
Collagen I	ab34710	Abcam	1 : 500	Proteinase K
Collagen III	ab7778	Abcam	1 : 500	Proteinase K
Decorin	BAF1060	R&D Systems	1 : 200	Chondroitinase ABC
LOX	ABT112	Millipore	1 : 300	Proteinase K
Lumican	n/a	Prof. Ake Oldberg	1 : 300	Proteinase K
Macrophages	MCA497G	Adb Serotec	1 : 1500	Proteinase K
Neutrophils	ab2557	Abcam	1 : 100	Proteinase K
NG2	MAB5384A4	Millipore	1 : 200	Proeinase K
PCNA	ab15497	Abcam	1 : 300	Proteinase K
PCNA (FITC)	PCNA01	Invitrogen	1 : 100	Proteinase K
ProSPC	ab90716	Abcam	1 : 2000	Proteinase K

Sources; Sigma-Aldrich, Schnelldorf, Germany; Abcam, Cambridge, UK; R&D Systems, Minneapolis, MN, USA; Professor Åke Oldberg, Lund University; Millipor, Temecula, CA, USA; Adb Serotech, Puchheim, Germany; Invitrogen Ltd, Paisley, UK.
Pretreatments; Proteinase K (P2308, Sigma-Aldrich) 20 μg/ml, 30 min, 37°C, Chondroitinase ABC (C2905, 0,5 IU/ml, Sigma), 1 h, 37°C.

magnification) to 10 (taken at 40× magnification). Analyses were performed slightly differently depending on the parameter studied:

PSR: Slides were viewed under polarized light at 40× magnification. The positively labelled area (μm^2) was calculated. The resulting data are given as positively stained area per total tissue area ($\mu m^2/mm^2$). Importantly, as the analysis was made using a dark background, the air spaces were not excluded in this analysis.
MTC: Large images of whole cross-sectioned lung were obtained at 4× (by taking several smaller images and stitching them together using the software NIS Elements, Nikon Instruments Inc., Melville, NY, USA), and a region of interest (ROI) was selected (lung parenchyma and distal lung were included whereas central lung including larger airways and vessels were excluded). Within this ROI the total tissue area (excluding airspaces) was measured. The area of a defined nuance of blue corresponding to the intense blue collagen staining was measured and related to the total tissue. The results are given as proportion collagen of the tissue (%). All lungs were inflated with PBS before sacrifice.
Tissue density: The fraction of tissue of total lung was determined using MTC-stained slides. This data is given as fraction tissue of total lung (%). Tissue density was also investigated by computerized counting of the number of DAPI-labelled nuclei. The data are given as number of nuclei/mm^2.
IHC: Depending on parameter, either the number of cells (Proliferation/PCNA and apoptosis/TUNEL) or the positively labelled area (collagen I, collagen III, LOX, decorin, biglycan and lumican) was calculated and related to image area.
Investigations of proliferating/apoptotic cell types: Double stainings were preformed on 1–2 animals/group and the number of double-positive cells analysed.

Statistical analysis. Results were statistically tested using Analyse-it for Microsoft Excel (Analyse-it Software, Ltd, Leeds, UK). For determination of statistical differences between the different groups the Kruskal-Wallis combined with the LSD *post hoc* test was performed, and all groups were compared pairwise. A p-value of <0.05 was considered statistically significant, and data is, if not stated otherwise, given as mean ± SD.

1. Tschumperlin, D. J., Liu, F. & Tager, A. M. Biomechanical regulation of mesenchymal cell function. *Curr Opin Rheumatol* **25**, 92–100 (2013).
2. Yeh, Y. T. *et al.* Matrix stiffness regulates endothelial cell proliferation through septin 9. *PloS one* **7**, e46889 (2012).
3. Perepelyuk, M. *et al.* Hepatic stellate cells and portal fibroblasts are the major cellular sources of collagens and lysyl oxidases in normal liver and early after injury. *Am J Physiol. Gastrointest liver physiol* **304**, G605–614 (2013).
4. Tilghman, R. W. *et al.* Matrix rigidity regulates cancer cell growth by modulating cellular metabolism and protein synthesis. *PloS one* **7**, e37231 (2012).
5. Bateman, E. D., Turner-Warwick, M. & Adelmann-Grill, B. C. Immunohistochemical study of collagen types in human foetal lung and fibrotic lung disease. *Thorax* **36**, 645–653 (1981).
6. Madri, J. A. & Furthmayr, H. Collagen polymorphism in the lung. An immunochemical study of pulmonary fibrosis. *Hum Pathol* **11**, 353–366 (1980).
7. Amenta, P. S., Gil, J. & Martinez-Hernandez, A. Connective tissue of rat lung. II: Ultrastructural localization of collagen types III, IV, and VI. *J Histochem cytochem* **36**, 1167–1173 (1988).
8. Perumal, S., Antipova, O. & Orgel, J. P. Collagen fibril architecture, domain organization, and triple-helical conformation govern its proteolysis. *Proc Acat Nat Sci U S A* **105**, 2824–2829 (2008).
9. Svensson, L. *et al.* Fibromodulin-null mice have abnormal collagen fibrils, tissue organization, and altered lumican deposition in tendon. *J Biol Chem* **274**, 9636–9647 (1999).
10. Shao, H. *et al.* Proteome profiling of wild type and lumican-deficient mouse corneas. *J Proteomics* **74**, 1895–1905 (2011).
11. Chakravarti, S. Functions of lumican and fibromodulin: lessons from knockout mice. *Glycoconj J* **19**, 287–293 (2002).
12. Tang, T. *et al.* Decreased Body Fat, Elevated Plasma Transforming Growth Factor-beta Levels, and Impaired BMP4-Like Signaling in Biglycan-Deficient Mice. *Connect Tissue Res* **54**, 5–13 (2012).
13. Schonherr, E. *et al.* Decorin deficiency leads to impaired angiogenesis in injured mouse cornea. *J Vasc Res* **41**, 499–508 (2004).
14. Robinson, P. S. *et al.* Influence of decorin and biglycan on mechanical properties of multiple tendons in knockout mice. *J Biomech Eng* **127**, 181–185 (2005).
15. Jepsen, K. J. *et al.* A syndrome of joint laxity and impaired tendon integrity in lumican- and fibromodulin-deficient mice. *J Biol Chem* **277**, 35532–35540 (2002).
16. Ameye, L. & Young, M. F. Mice deficient in small leucine-rich proteoglycans: novel in vivo models for osteoporosis, osteoarthritis, Ehlers-Danlos syndrome, muscular dystrophy, and corneal diseases. *Glycobiology* **12**, 107R–116R (2002).
17. Zheng, Z. *et al.* Delayed wound closure in fibromodulin-deficient mice is associated with increased TGF-beta3 signaling. *J Invest Dermatol* **131**, 769–778 (2011).
18. Oldberg, A. *et al.* Collagen-binding proteoglycan fibromodulin can determine stroma matrix structure and fluid balance in experimental carcinoma. *Proc Natl Acad Sci U S A* **104**, 13966–13971 (2007).
19. Rydell-Tormanen, K. *et al.* Extracellular matrix alterations and acute inflammation; developing in parallel during early induction of pulmonary fibrosis. *Lab Invest* **92**, 917–925 (2012).
20. Iozzo, R. V. & Schaefer, L. Proteoglycans in health and disease: novel regulatory signaling mechanisms evoked by the small leucine-rich proteoglycans. *FEBS J* **277**, 3864–3875 (2010).
21. Westergren-Thorsson, G. *et al.* Lung fibroblast clones from normal and fibrotic subjects differ in hyaluronan and decorin production and rate of proliferation. *Int J Biochem Cell Biol* **36**, 1573–1584 (2004).
22. Schaefer, L. *et al.* Biglycan, a nitric oxide-regulated gene, affects adhesion, growth, and survival of mesangial cells. *J Biol Chem* **278**, 26227–26237 (2003).
23. Nastase, M. V., Young, M. F. & Schaefer, L. Biglycan: a multivalent proteoglycan providing structure and signals. *J Histochem Chytochem* **60**, 963–975 (2012).
24. Shami, A. *et al.* Fibromodulin deficiency reduces low-density lipoprotein accumulation in atherosclerotic plaques in apolipoprotein E-null mice. *Arterioscler Thromb Vasc Biol* **33**, 354–361 (2013).
25. Ameye, L. *et al.* Abnormal collagen fibrils in tendons of biglycan/fibromodulin-deficient mice lead to gait impairment, ectopic ossification, and osteoarthritis. *FASEB* **16**, 673–680 (2002).

Acknowledgments

The authors would like to express their sincere gratitude towards Åke Oldberg and Sebastian Kalamajski for the fibromodulin-deficient mice and sharing unpublished data on these animals, to Tore Saxne and Dick Heinegård for participation in designing the study,

Marie Wildt for technical assistance and Jenny Karlsson for technical and administrative help. This work was made possible by grants from The Royal Physiographic Society, Swedish Research Counsel (Grant number: 11550), Swedish Heart-Lung Foundation, Kock's Foundation, Lars Hiertas Memorial Foundation, Österlund's Foundation, Gyllenstierna Krapperup's Foundation, The Sandberg Foundation and Faculty of Medicine, Lund University.

Author contributions

K.R.T. designed the study, carried out animal experiments, performed and analysed the immunohistochemistry, analysed results and drafted the manuscript. K.A. participated in the animal experiments and helped drafting the manuscript. R.H. participated in the study design and helped drafting the manuscript. G.W.T. participated in the study design, interpretation of data and helped drafting the manuscript. All authors read and approved of the final manuscript.

Additional information

Supplementary information accompanies this paper at http://www.nature.com/scientificreports

Competing financial interests: The authors declare no competing financial interests.

How to cite this article: Rydell-Törmänen, K., Andréasson, K., Hesselstrand, R. & Westergren-Thorsson, G. Absence of fibromodulin affects matrix composition, collagen deposition and cell turnover in healthy and fibrotic lung parenchyma. *Sci. Rep.* **4**, 6383; DOI:10.1038/srep06383 (2014).